Binding energy and monolayer capacity of Xe on single-wall carbon nanotube bundles

A. J. Zambano, S. Talapatra, and A. D. Migone
Department of Physics, Southern Illinois University, Carbondale, Illinois 62901
(Received 26 February 2001; published 26 July 2001)

We have determined the adsorptive capacity of Xe on the different groups of binding sites available to this atom on a sample of single-walled carbon nanotube (SWNT) bundles. The SWNT's used were not treated after production: hence, the caps at the ends of each of the tubes remain intact. By comparing these experimental values to the values computed for the different portions of the bundles obtained from geometrical considerations, we conclude that Xe adsorption takes place only on the outer surfaces of the SWNT bundles. We have also measured Xe adsorption isotherms on the same SWNT sample at a low coverages for nine different temperatures (between 210 and 295 K) to determine the isosteric heat of adsorption of Xe on the SWNT's; this quantity is directly related to the binding energy of the adsorbate to the substrate. We determined that the binding energy of Xe on the SWNT's is 282 ± 11 meV. This value is 74% larger than that for Xe on planar graphite.

DOI: 10.1103/PhysRevB.64.075415 PACS number(s): 61.48.+c

INTRODUCTION

The study of the adsorption of gases on carbon nanotubes has been attracting considerable interest recently.[1–14] A number of studies, experimental[1–9] as well as theoretical,[10–14] have been conducted on these systems. Interest in adsorption on nanotubes stems in part from fundamental considerations, since systems formed by gas adsorption on nanotubes can provide experimental realizations of matter in one dimension.[6,8,12] There are very strong practical motivations, as well, for studying adsorption on nanotubes. Gases adsorbed on nanotubes have the potential of revolutionizing gas storage technology[3] and gas distillation processes.[15]

Xe is being increasingly used in the automotive industry in headlights for automobiles. This provides a strong economic incentive for finding new and efficient ways of distilling this rare gas from air. Xe is only present at 0.08 ppm in air; its separation from air's other components is carried out in several consecutive steps.[16] In the last one of these, a mixture of Kr and Xe is separated by solidifying the mixture at liquid-nitrogen temperatures and using the difference between the vapor pressures to extract essentially pure Kr from the vapor, leaving a Xe-rich solid residue.[16] Provided that Xe has a sufficiently large binding energy on the single-walled carbon nanotubes (SWNT's), this last purification step could be replaced with a room-temperature, Xe-capturing SWNT filter.

A SWNT can be viewed as a single graphene sheet rolled over itself and closed seamlessly, with its ends capped.[17] SWNT's assemble into bundles.[18,19,20] Theoretical studies have identified three different types of adsorption sites in close-ended SWNT bundles:[14] (i) the cylindrical outer surfaces of the individual nanotubes that lie at the external surface of the bundles, (ii) the region where two of these external tubes come close together, i.e., the outer ''grooves'' on the surface of the bundle, and (iii) the space in between the individual nanotubes at the interior of the bundle, i.e., the interstitial channels (IC's). A schematic of a cross section of a nanotube bundle indicating these three different groups of sites is shown in Fig. 1. The grooves and cylindrical outer surfaces of the individual nanotubes constitute the external surface of the bundles. Computational results for ^{4}He and Ne (which the calculations expect to be sufficiently small to fit in the IC's) find that the groove sites have stronger binding energy than planar graphite, but weaker than the IC's.[14] The least attractive of the three groups of sites, those on the outside surface of individual nanotubes located at the outside of a bundle, have binding energies which are smaller than those for adsorption on planar graphite.[14] This sequence of binding energies can be understood in terms of the following simple argument. For an atom capable of penetrating into the IC's, the large number of C atoms near every adsorption site would result in a considerably larger binding energy than that

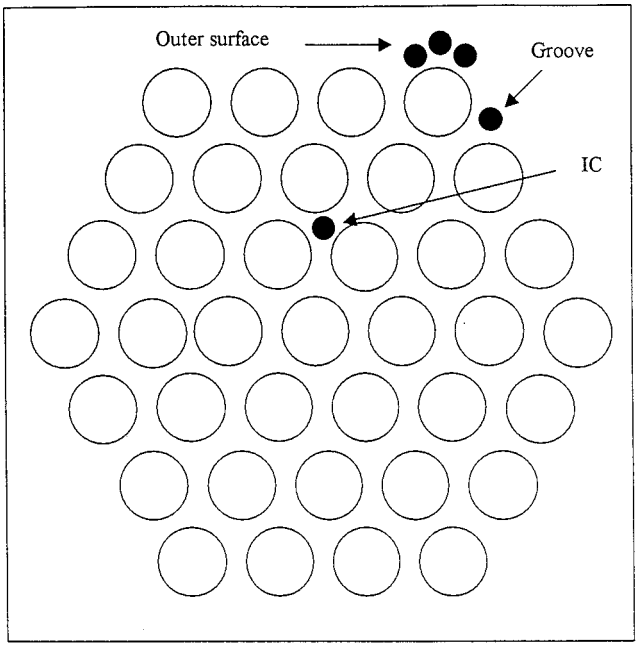

FIG. 1. Schematic drawing of the three groups of adsorption sites on a nanotube bundle. The groove sites and the external surface sites are available for adsorption in all cases, regardless of the size of the adsorbate. Whether or not the IC's are available for adsorption by any gas is at present a matter of considerable research activity.

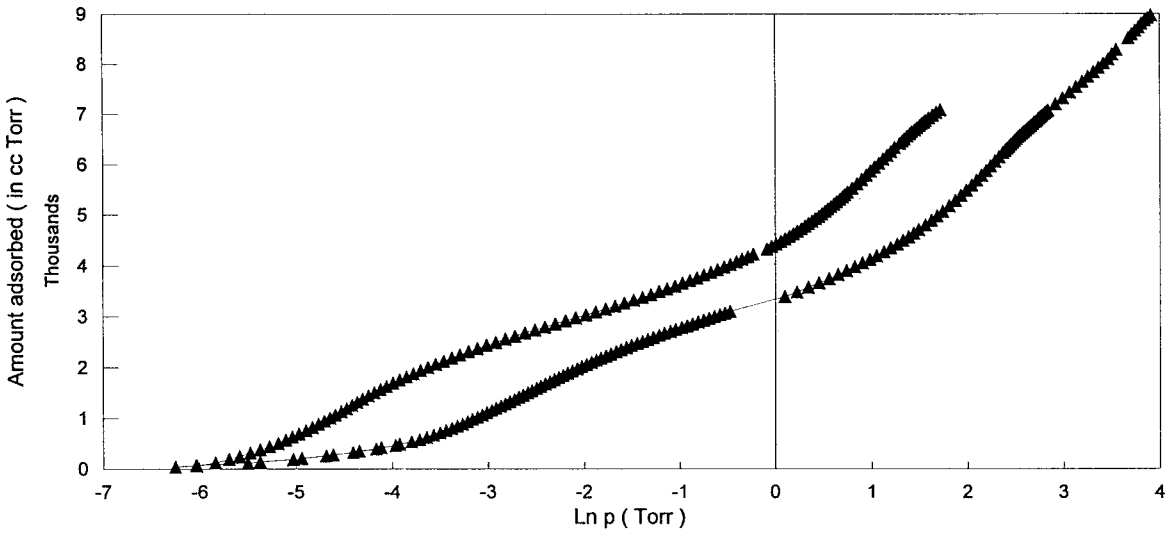

FIG. 2. Adsorption isotherms at 138 and 150 K. The amount of gas adsorbed is given in cm^3 Torr and plotted in the *y* axes as a function of the logarithm of the pressure (in Torr) which is plotted in the *x* axes. Here 1 cm^3 Torr at 273 is equivalent to 58.8 nanomoles.

available on planar graphite.[11,12,14] Similarly, the number of C atoms near each site in the outer grooves is greater than on planar graphite, but smaller than on the IC's, resulting in intermediate binding energies for the ridge sites.

In this paper we report on an experimental determination of the isosteric heat of adsorption, q_{st}, and of the binding energy ε of Xe adsorbed on SWNT's. Both of these quantities were determined from adsorption isotherm data measured at low coverages.

Nanotubes form a triangular array in the bundles. While there is some spread in the value of the tube diameters, they are peaked around 13.8 Å and the intertube separation is peaked around 17 Å.[17,18,19,20] Based on purely geometrical considerations (and assuming a perfectly narrow distribution for the diameters), the largest sphere that could fit in an IC would have a diameter of 0.58 nm. However, this value significantly overestimates the diameter which is actually accessible for adsorption, since it ignores the electronic clouds associated with each of the tubes forming the IC's. The actual diameter available for adsorption in an IC can be estimated by assuming that the electronic clouds have a size comparable to the separation between basal planes in graphite, i.e., 3.4 Å.[21] Subtracting this value from the geometric diameter, we obtain that the diameter available for adsorption in the IC's is approximately 0.26 nm. We have assumed in these considerations that the bundles are rigid, i.e., that the intertube separation remains fixed and no ''swelling'' of the bundles occurs; this is quite reasonable for larger adsorbates, such as Xe.

Estimates for the adsorptive capacity of a specific sample of close-ended SWNT, as well as estimates for the adsorptive capacities of each of the three sets of adsorption sites can be obtained by combining information on the weight and purity of the sample with simple geometric considerations. Comparing the results of these geometrical estimates to the experimental adsorption data provides a reasonable, if indirect, approach for determining which type of sites are available for adsorption for a given species. We present below the results of two Xe adsorption isotherms which were used to conduct precisely this type of comparison.

EXPERIMENT

The SWNT samples utilized in this study were prepared by electric arc discharge; details are provided elsewhere.[19] The SWNT's were not subjected to any post-production treatment; hence, the ends of the tubes are capped. The reported purity of the samples produced by the arc discharge method is on the order of 80% by weight.[19]

The mass of the nanotube-containing sample was 0.290 ± 0.0005 g. The nanotubes were kept in a container open to atmosphere. The sample was placed in a copper cell and evacuated to a pressure below 1×10^{-6} Torr for a period of at least 12 h at room temperature prior to the performance of the adsorption measurements. The adsorption isotherm apparatus used has been described previously.[22]

The low-coverage adsorption measurements were conducted at nine different temperatures between 210 and 295 K. Low coverages and high binding energies result in relatively low pressures. All the pressures used in the isosteric heat determination were measured with either a 1-Torr or a 10-Torr full-scale gauge. We applied thermomolecular corrections to all the data.[23] This correction takes into account differences between actual and measured values when the pressure is determined for a low-temperature location by a room-temperature gauge.[23] The correction was, in all cases considered here, less than 10% of the uncorrected value.

RESULTS

We have measured Xe adsorption isotherms at 138 and 150 K (both of these temperatures are below the bulk triple point of Xe, $T_t \approx 164.5$ K). In Fig. 2, which displays these data, the amount of Xe adsorbed on the substrate in cm^3 Torr (1 cm^3 Torr at 273 K is equivalent to 58.8 nanomoles) is

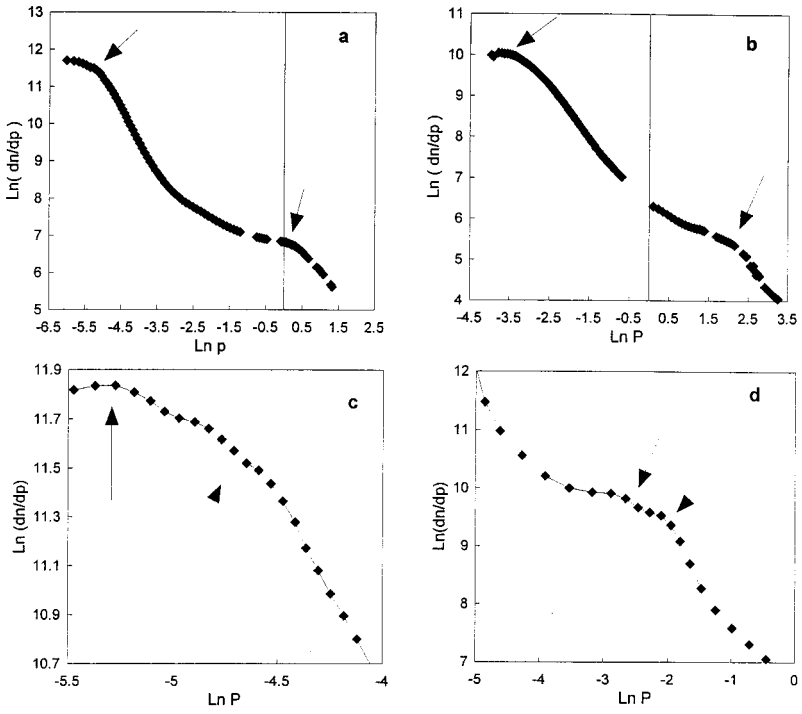

FIG. 3. Logarithm of the 1D isothermal compressibility per unit effective one-dimensional length of the film plotted as a function of the logarithm of the pressure. Compressibility for the complete (a) 138-K and (b) 150-K isotherms. The two broad compressibility peaks correspond to the two isotherm steps. (c) Highly expanded view of the compressibility in the region corresponding to the lower-pressure step at 138 K. Two closely spaced compressibility peaks comprise this low-pressure feature. (d) Expanded plot of the compressibility in the coverage region corresponding to the higher-pressure step for data measured at 115 K. Two closely spaced peaks are present.

presented on the y axis as function of the logarithm of the pressure (in Torr).

For a fixed temperature, the logarithm of the pressure is directly proportional to the chemical potential of the film. On a substrate characterized by several sets of well-defined binding energies (as should be, roughly, the case for nanotube bundles), adsorption on a given set of sites takes place at a nearly constant value of the chemical potential. Hence the choice of axes in Fig. 2 is apt to reveal adsorption occurring on the different groups of adsorption sites as steps in the data. This is indeed the case here. There are two, somewhat rounded, steps present. The first one starts at zero coverage and ends at about 2000 cm^3 Torr; the second ends at a coverage of about 7200 cm^3 Torr. The midpoint of the first step occurs at about 0.01 Torr ($\ln P=-4.605$) for the 138-K and at about 0.06 Torr ($\ln P=-2.813$) for the 150-K isotherm. The midpoint of the second step in the data occurs near 2.2 Torr ($\ln P=0.788$) at 138 K and near 9.5 Torr ($\ln P=2.251$) at 150 K. For comparison, an estimate of the pressure at the midpoint of the first layer for Xe on planar graphite[24] at 138 K (calculated using values derived from lower temperatures) is 0.28 Torr ($\ln P=-1.273$) and it is 1.25 Torr ($\ln P=0.223$) at 150 K. That is, the pressure at the midpoint of the first layer for Xe on graphite is greater than the value of the pressure of the first step on the SWNT's and smaller than the value of the second step for Xe on the SWNT's for the same temperature.

In Figs. 3(a) and 3(b) we display the derivative of the adsorption data as a function of pressure for the two isotherms displayed in Fig. 2. This quantity is directly proportional to the isothermal compressibility of the film. There are two broad maxima present in Fig. 3(a), indicated by arrows. Each maximum corresponds to a broad step in Fig. 2.

A more careful look at the compressibility data in Figs. 3(a) and 3(b) shows that each one of the two broad peaks, in turn, possesses some structure. In Fig. 3(c) we present a much expanded view of the derivative of the adsorption data in the region corresponding to the lower-pressure peak for the 138-K data. There are two closely spaced peaks at slightly different pressures. A similar behavior is present in the data for the higher pressure step. In Fig. 3(d) we present the derivative of the adsorption data for coverages corresponding to that of the higher-pressure step for isotherms measured at lower temperature (115 K). The same features in the second step are also present at 138 and 150 K, although for these higher temperatures they are harder to resolve. Each of the two pairs of closely spaced compressibility maxima associated with the two isotherm steps corresponds to two subsets of sites with close, but slightly different, binding energies

ISOSTERIC HEAT AND BINDING ENERGY RESULTS

We have performed low-coverage adsorption isotherm measurements at nine different temperatures to determine the isosteric heat of Xe on the high-energy sites in the nanotube bundles. In Fig. 4 we present, plotted in a semilogarithmic scale all the adsorption data measured for the nine temperatures investigated between 210 and 295 K. The amount of Xe adsorbed (y axis) is plotted as a function of the logarithm of the pressure (x axis). Note that the entire range of coverages utilized in these isosteric heat determinations is less than one-fifth of the value corresponding to the first step.

The isosteric heat of adsorption, q_{st}, is the amount of heat released when an atom adsorbs on a substrate.[25] It can be determined from adsorption isotherm data measured at different values of the temperature by using the following expression:[25]

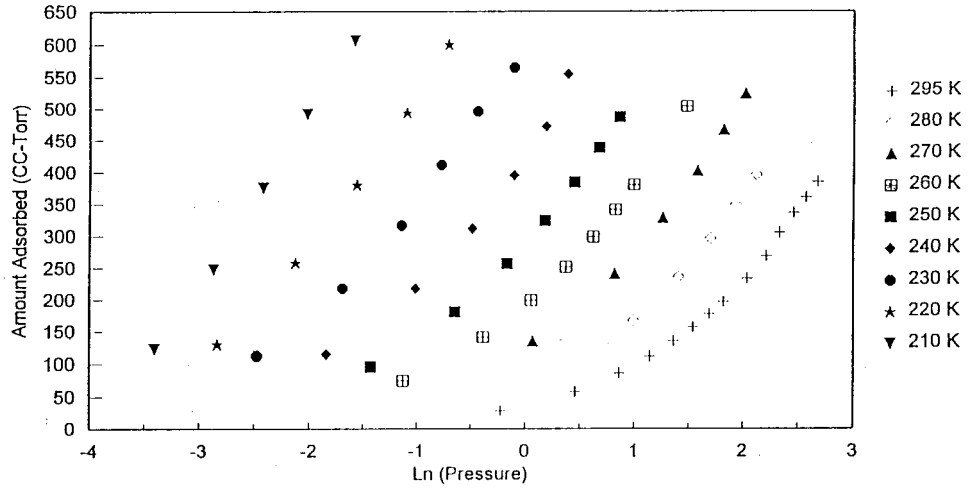

FIG. 4. Low-coverage adsorption data. Note that the entire span of coverages shown is less than one-fifth of the amount corresponding to the lower-pressure step. Plotted, from left to right, are data for 210, 220, 230, 240, 250, 260, 270, 280, and 295 K.

$$q_{st} = kT^2[\partial \ln(P)/\partial T]_\rho . \quad (1)$$

Here, k is Boltzmann's constant, ρ is the one-dimensional (1D) density of the adsorbed gas in the nanotubes, $\ln(P)$ is the logarithm of the pressure of the coexisting 3D gas (which is present in the vapor phase inside the cell), and T is the average value of the temperature. In practice, the derivatives are approximated by differences between data points in isotherms measured at different temperatures for the same value of the amount adsorbed.

Our results for the isosteric heat are presented in Table I. The entries in this table were calculated for a selected set of values for the amount adsorbed (150, 200, 250, 300, 350, 400, 450, 500, and 550 cm^3 Torr). For each value of the amount adsorbed, all possible pairs of temperatures were formed (210 and 220 K, 210 and 230 K, etc.). Then the q_{st} was determined for each amount adsorbed and each pair of temperatures. An average q_{st} value corresponding to each amount adsorbed was then obtained. Finally, the average value of all these q_{st}'s was calculated.

TABLE I. Values of isosteric heat of adsorption (in meV) determined for selected values of the amount adsorbed. For each coverage q_{st} was calculated as the average value obtained using all the possible different pairs of temperatures. The overall average q_{st} value for Xe on the SWNT's was calculated as the average of the q_{st} values for the different selected coverages.

Coverage (cm^3 Torr)	q_{st} (meV)	Uncertainty (meV)
150	327	16
200	328	15
250	330	11
300	328	9
350	326	9
400	320	10
450	330	7
500	329	9
550	315	6
Average	326	10

As was discussed in greater detail elsewhere,[2] the relation between the isosteric heat and binding energy for a one-dimensional adsorbed film is given by

$$q_{st} = \varepsilon + 2kT. \quad (2)$$

In Table I we present the values of the binding energies calculated from the average values of q_{st}. The average value obtained from all the pairs of temperatures for the binding energy of methane on the carbon nanotube bundles is $\varepsilon = 282 \pm 11$ meV. As a point of comparison, the reported value of the binding energy for xenon on planar graphite is 162 ± 4 meV.[26] The value of the binding energy measured on the SWNT's is 74% larger than on planar graphite.

DISCUSSION

We performed a geometrical calculation to estimate the amount of Xe adsorbed on each of the three groups of sites on close-ended SWNT bundles. We assumed, for simplicity, that the nanotubes form hexagonal bundles and that all the nanotubes were 1500 Å in length and 13.8 Å in diameter with both ends closed. We calculated the amount of Xe adsorbed for bundles of 19, 37, 91, 169, and 217 nanotubes. The weight of each nanotube was computed by adding the weight of all C atoms present on the nanotube. The total number of bundles in the sample was calculated by dividing the total weight of the sample by the weight of each bundle.

The amount adsorbed on each bundle was obtained by adding the amounts adsorbed on each of the different types of sites mentioned in the Introduction: IC's, grooves, and external surface. The amount adsorbed on the grooves was calculated by dividing the length of a nanotube by the diameter of a Xe atom and multiplying it by the number of grooves in each bundle. Similarly, assuming that Xe can go into the IC's, the number of Xe atoms that would be adsorbed on the IC's if this were possible was calculated by

TABLE II. Geometric calculation of the maximum total possible number of Xe atoms adsorbed at monolayer completion for SWNT samples constituted by identical bundles. Five different sizes were used: bundles with 19, 37, 91, 169, and 217 tubes in them, respectively. For each bundle size, the number of Xe atoms adsorbed was calculated assuming two different scenarios: either that Xe cannot adsorb on the IC's or that it can adsorb in these regions. The percentages of the atoms adsorbed in each of the three groups of sites (respectively, IC's, grooves, and cylindrical outer surfaces of individual nanotubes at the outer surface of the bundles) are presented for each of the two scenarios. The final entry in the table is the experimentally measured data.

SWNT's/ Bundle	Amt. Ads. (Number of atoms)	Interstitial Channels (%)	Grooves (%)	Outer Surface (%)
19				
Without IC's	4.46×10^{20}	0	21	79
With IC's	6.33×10^{20}	29	15	56
37				
Without IC's	3.26×10^{20}	0	22	78
With IC's	5.4×10^{20}	40	13	47
91				
Without IC's	2.1×10^{20}	0	23	77
With IC's	4.6×10^{20}	53	11	36
169				
Without IC's	1.8×10^{20}	0	23	77
With IC's	4.3×10^{20}	58	10	32
217				
Without IC's	1.6×10^{20}	0	23	77
With IC's	4.2×10^{20}	61	9	30
Experiment	2.5×10^{20}	0	25	75

dividing the length of an IC by the Xe diameter and multiplying this by the number of IC's present in each bundle. The number of Xe atoms on the external surface sites was estimated by adding the outer area of each cylinder at the outer surface of the bundle, subtracting from this sum the portion of the area covered by the Xe in the grooves, and dividing the resulting area by the area of the triangular unit cell of planar Xe.

For each of the five bundle sizes used, we considered two possibilities: that the IC's contributed to the adsorption and that they did not. The results are presented in Table II. They show that the fraction adsorbed in each type of site, for each of two possibilities, is substantially independent of the number of nanotubes per bundle in the range of bundle sizes investigated here.

The first point to be noted when comparing the geometrical calculations with experiment is that if Xe were adsorbing on the IC's, as well as on the grooves and external surfaces of the outside tubes, we would expect to find three steps in the isotherms: one for the IC's, one for the grooves, and one for the outer surfaces.

The fact that only two steps are present in the data (see Fig. 2), one below and one above the pressure for the first layer of Xe on graphite, indicates that there only are two groups of sites available for adsorption for Xe: one more tightly bound and one less tightly bound than the first layer of Xe on planar graphite.

In the experimental data displayed in Fig. 2, the top of the first step occurs at a coverage of about 2000 cm^3 Torr for both 138 and 150 K. The top of the second step occurs at about 7200 cm^3 Torr in both cases. The ratio of the amounts adsorbed in these two regions is approximately 2.6 to 1. The lower-pressure step corresponds to the stronger binding sites. The result of our geometrical calculations (see Table II) shows that the when one considers the grooves to be the only high-energy binding sites available for adsorption, the Xe adsorbed in these high-energy ridge sites bears a ratio of 3:1 with respect to the amount adsorbed on the outside surface. This result is in reasonably good agreement with that obtained in the measurements.

From the fact that only two steps are observed and from the agreement between the geometrical calculation and the experimental data, we conclude that Xe atoms adsorb exclusively on the external surfaces of the bundles (i.e., on the grooves and on the outer cylindrical surfaces of the individual nanotubes).

By comparing our result for the number of atoms adsorbed at layer completion obtained in the experiment to the geometrical calculation (which was performed assuming a sample purity of 80%),[19] we can arrive at our own estimate for the purity of the sample. The measured number of atoms adsorbed corresponds to 80% of the geometrical calculation. This yields a purity estimate for the sample of 60% by weight.

While the amount of impurities present is rather a rather large weight fraction of the sample, we note that the most important consideration form the perspective of adsorption isotherms is the fraction of the surface area in the substrate sample that is provided by the impurities, not their fractional weight. Further, it has been noted[19,20] that the most significant impurities by weight are amorphous carbon and the metallic catalyst residue. The metallic particles are found embedded in amorphous carbon.[19,20] Amorphous carbon will bind rare gases less strongly than the grooves of the nanotube bundles, so the presence of these impurities will have little effect on the binding energy values determined. In addition, amorphous carbon will not produce any resolvable features in an adsorption isotherm; it will just add a smooth background contribution to the adsorption. The specific area provided both by the amorphous carbon as well as the metallic catalyst residue is very small when compared to the specific area of the nanotubes in the sample. As a result of these considerations, we expect the principal effect of the impurities to be a decrease the specific area of the sample.

The main result of the isosteric heat measurements is our finding that the binding energy of Xe on the SWNT bundles, 282 meV, is 1.74 times the value of the corresponding quantity on planar graphite. Since the Xe atoms are limited to adsorb on the external ridges on the surface of the bundles and on the external cylindrical surfaces of individual tubes in our closed-ended sample, we conclude that the groove sites are the high-energy sites for which we have determined the binding energy. We note that very similar increases have

been determined for Ne and CH_4 adsorbed on SWNT substrates.[2,7]

It is interesting to compare the value we have determined for the binding energy on the grooves to very recent theoretical estimates for this quantity.[14] The theoretical calculations find an increase of approximately 70% in the groove binding energy value over the value determined for the same adsorbate on a sheet of planar graphite.[14]

A recent adsorption study of CH_4 and Kr on SWNT samples, which possesses essentially the same qualitative characteristics as the data we have presented here for Xe, was interpreted in terms of adsorption in the interstitial spaces.[9] It should be noted, however, that in that study the existence of groove sites in the nanotube bundles was completely ignored; hence, the groove sites were not considered as a possible source for the lower-pressure steps.[9] Neglect of the existence of groove sites limited the identification of the two features in the adsorption isotherm just to IC's and external surfaces, and led to the incorrect identification of the features in the data.[9]

CONCLUSIONS

From a comparison between monolayer adsorption results for Xe determined from isotherm measurements and those obtained from simple geometrical calculations, we conclude that Xe adsorbs only on the outer surface of the SWNT bundles. We have determined that the binding energy of Xe on the high-energy binding sites available on the grooves on the external surface of the bundles has a value of 282 ± 11 meV. This binding energy value is 74% larger than that found for the same adsorbate on planar graphite. The measured increase in binding energy in the ridge sites over the value on planar graphite is in agreement with the increase obtained in theoretical calculations.

ACKNOWLEDGMENTS

A. D. M. would like to acknowledge support by the Research Corporation through a Cottrell award, the donors of the Petroleoum Research Fund of the American Chemical Society for partial support of this work, and the National Science Foundation through Grant No. DMR-0089713 for supporting this work. We would like to thank Professor Milton W. Cole, Dr. George Stan, and Dr. Silvina Gatica for a number of illuminating comments, as well as for having made available to us their results prior to publication. We would especially like to thank Professor Samuel C. Fain, Jr. for a very careful reading our original manuscript and for his numerous and incisive comments on it.

[1] E. B. Mackie, R. A. Wolfson, L. M. Arnold, K. Lafdi, and A. D. Migone, Langmuir **13**, 7197 (1997).
[2] S. E. Weber, S. Talapatra, C. Journet, A. J. Zambano, and A. D. Migone, Phys. Rev. B **61**, 13 150 (2000).
[3] A. C. Dillon, K. M. Jones, T. A. Bekkedahl, C. H. Kiang, D. S. Bethune, and M. J. Heben, Nature (London) **386**, 377 (1997).
[4] S. Inoue, N. Ichikuni, T. Suzuki, T. Uematsu, and K. Kaneko, J. Phys. Chem. B **102**, 4690 (1998).
[5] C. Nutzenadel, A. Zuttel, D. Chartouni, and L. Schlapbach, Electrochem. Solid State Lett. **2**, 30 (1999).
[6] W. Teizer, R. B. Hallock, E. Dujardin, and T. W. Ebbesen, Phys. Rev. Lett. **82**, 5305 (1999); W. Teizer, R. B. Hallock, E. Dujardin, and T. W. Ebbesen, *ibid.* **84**, 1844(E) (2000).
[7] S. Talapatra, A. J. Zambano, S. E. Weber, and A. D. Migone, Phys. Rev. Lett. **85**, 138 (2000).
[8] A. Kuznetsova, J. T. Yates, Jr., J. Liu, and R. E. Smalley, J. Chem. Phys. **112**, 9590 (2000); A. Kuznetsova, D. B. Mawhinney, V. Naumenko, J. T. Yates, J. Liu, and R. E. Smalley, Chem. Phys. Lett. **321**, 292 (2000).
[9] M. Muris, N. Dufau, M. Bienfait, N. Dupont-Pavlosky, Y. Grillet, and J. P. Palmari, Langmuir **16**, 7019 (2000).
[10] G. Stan and M. W. Cole, J. Low Temp. Phys. **110**, 539 (1998).
[11] G. Stan, V. H. Crespi, M. W. Cole, and M. Boninsegni, J. Low Temp. Phys. **113**, 447 (1998).
[12] G. Stan, S. Gatica, M. Boninsegni, S. Curtarolo, and M. W. Cole, Am. J. Phys. **67**, 1170 (1999).
[13] G. Stan and M. W. Cole, Surf. Sci. **395**, 280 (1998).
[14] G. Stan, M. J. Bojan, S. Curtarolo, S. M. Gatica, and M. W. Cole, Phys. Rev. B **62**, 2173 (2000).
[15] Alan C. Cooper (private communication).
[16] N. A. Downie, *Industrial Gases* (Blackie Academic & Professional, London, 1997).
[17] A number of recent reviews have appeared in articles and in books on the subject of carbon nanotubes; see, for example, P. M. Ajayan and T. W. Ebbesen, Rep. Prog. Phys. **60**, 1025 (1997) or *Physical Properties of Carbon Nanotubes*, R. Saito, G. Dresselhaus and M. S. Dresselhaus (Imperial College Press, London, 1998).
[18] C. H. Kiang, W. A. Goddard, R. Beyers, and D. S. Bethune, Carbon **33**, 903 (1995); C. H. Kiang, W. A. Goddard, R. Beyers, J. R. Salem, and D. S. Bethune, J. Phys. Chem. Solids **57**, 35 (1996).
[19] C. Journet, W. X. Maser, P. Bernier, M. Lamy de la Chapelle, S. Lefrants, P. Deniards, R. Lee, and J. E. Fischer, Nature (London) **388**, 756 (1997).
[20] A. Thess, R. Lee, P. Nikolaev, H. Dai, P. Petit, J. Robert, C. Xu, Y. H. Lee, S. G. Kim, A. G. Rinzler, D. T. Colbert, G. E. Scuseria, D. Tomanek, J. E. Fischer, and R. E. Smalley, Science **273**, 483 (1996).
[21] R. W. G. Wyckoff, *Crystal Structures*, 2nd ed. (Interscience, New York, 1965), Vol. 1.
[22] P. Shrestha, M. T. Alkhafaji, M. M. Lukowitz, G. Yang, and A. D. Migone, Langmuir **10**, 3244 (1994); R. A. Wolfson, L. M. Arnold, P. Shrestha, and A. D. Migone, *ibid.* **12**, 2868 (1996).
[23] T. Takaishi and Y. Sensui, Trans. Faraday Soc. **53**, 2503 (1963).
[24] A. Thomy and X. Duval, J. Chim. Phys. (Paris) **67**, 1101 (1970).
[25] J. G. Dash, *Films on Solid Surfaces* (Academic Press, New York, 1975).
[26] G. Vidali, G. Ihm, H.-Y. Kim, and M. W. Cole, Surf. Sci. Rep. **12**, 133 (1991).